ORIGINAL PAPER

New Catalytic Materials for the Direct Epoxidation of Propylene by Oxygen: Application of High-Throughput Pulsed Laser Ablation

Michael Kahn · Anusorn Seubsai · Isik Onal · Selim Senkan

Abstract New catalytic materials were prepared by depositing nanoparticles of 35 different metals as well as their select binary combinations on Al_2O_3, CeO_2, SiO_2, TiO_2, and ZrO_2 supports. Nanoparticles were synthesized by high-throughput pulsed laser ablation (PLA). Catalytic materials were then screened for their selectivities towards the synthesis propylene oxide (PO) from propylene and oxygen using array channel microreactors at 1 atm and 300, 333, and 367 °C. A gas hourly space velocity (GHSV) of 20,000 h^{-1} was used at the feed gas composition of 20% O_2, 20% C_3H_6 and the balance He. Initial screening experiments resulted in the discovery of SiO_2 supported Cr, Mn, Cu, Ru, Pd, Ag, Sn, and Ir as the most promising leads for PO synthesis. Subsequent experiments pointed to bimetallic Cu-on-Mn/SiO_2, for which the PO yields increased several fold over single metal catalysts. For multimetallic materials, the sequence of deposition of the active metals was shown to have a significant effect on the resulting catalytic activity and selectivity.

Keywords Partial oxidation · Nanoparticle synthesis · Multimetallic catalysis

M. Kahn · A. Seubsai · S. Senkan (✉)
Department of Chemical Engineering, UCLA, Los Angeles, CA 90095, USA
e-mail: ssenkan@gmail.com

I. Onal
Chemical Engineering Department, Middle East Technical University, Ankara, Turkey

1 Introduction

Propylene oxide (PO) is an important intermediate produced over 10 billion pounds per year using two major technologies—the chlorohydrin and hydroperoxide processes [1]. However, both of these processes are laden with serious economic, health and environmental drawbacks. The chlorohydrin process requires the use of chlorine, which is a toxic and corrosive reagent, and can produce additional toxic chlorinated organic by-products. The hydroperoxide process produces co-products, such as the styrene monomer, thereby linking the economic viability of PO production to the market value of the co-product. Recently, a new PO synthesis route based on the in situ production of H_2O_2 is also being commercialized [2]. Nevertheless, the direct synthesis of PO from propylene and molecular oxygen remains one of the most challenging goals of industrial catalysis.

To date, a large variety of heterogeneous and homogeneous catalysts, and in particular supported metal catalysts have been investigated for the title reaction using different techniques. [3-17, also 2 and references therein] Notably, silver and palladium were explored [3–6], but the most attention has been given to gold nanoparticles, e.g. Au/TiO_2 and Au/TS-1 [2, 4, 7–13]. The latter was shown to exhibit high selectivity (50–90%) towards PO production. However, gold catalysts utilize hydrogen as a co-reactant for PO synthesis, rendering this process less desirable for industrial implementation. Most recently, copper was reported to be effective in the direct production of PO, without hydrogen, although the initial yields were below those required for commercial interest [14, 15].

The lack of a breakthrough in propylene epoxidation catalysis, in spite of world-wide efforts, clearly suggests the need to develop novel approaches for catalyst research

and development. This fact, coupled with the abundance of catalytic materials that must be explored to discover new leads, e.g. binary, ternary and higher order combinations of metals as well as a large variety of support materials, call for the application of combinatorial or high throughput heterogeneous catalysis tools and methods. Our laboratories made pioneering contributions to this field through the development of novel high-throughput catalyst preparation and screening tools [18–22]. In particular, we developed array channel micro-reactors to rapidly screen a large numbers of catalytic materials in parallel [18, 19]. In addition, we coupled these array reactors to laser spectroscopy [18], photoionization detection (PID) [18], mass spectrometry [20], and fast gas chromatography [21]. Recently, we also developed a high-throughput pulsed laser ablation (HT-PLA) system for the synthesis of uniformly sized single- and multi-metallic nanoparticles for catalytic applications [22].

Here we report on the results of a comprehensive and systematic investigation of the catalytic properties of supported nanoparticles of 35 different metals prepared by HT-PLA for the direct synthesis of PO from propylene and oxygen. The direct epoxidation of propylene by oxygen involves the following overall stoichiometry:

$$C_3H_6 + \frac{1}{2}O_2 \rightarrow C_3H_6O$$
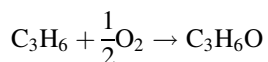
However, besides PO, the partial oxidation of propylene can also form a variety of by-products such as acetone (AT), acrolein (AC), acetaldehyde (AD), and propanal (PaL, usually trace), together with deep oxidation products of CO and CO_2. The challenge in catalysis is to maximize PO production while minimizing the formation of all the by-products while attaining useful propylene conversions. Initial screening experiments resulted in both confirmatory findings (e.g. Cu, Ag, and Pd) and new discoveries of SiO_2 supported Cr, Mn, Ru, Sn, and Ir. Subsequent studies of the bimetallic Mn and Cu system, also supported on SiO_2 has led to a remarkable improvement of the PO yield, by nearly a factor of 5 when compared to single-component catalysts. These findings not only suggest the use of multi-metallic systems for direct propylene epoxidation catalysis, but also provide a clear demonstration of the utility of high-throughput techniques for catalyst discovery and optimization.

2 Experimental

Catalytic materials were prepared by depositing nanoparticles of metals on standard pellets of gamma-Al_2O_3 (23.4 mg pellet weight, 128 m^2/g BET area), CeO_2 (61 mg, 17 m^2/g), SiO_2 (9.6 mg, 398 m^2/g), TiO_2 (anatase,

11.7 mg, 268 m^2/g) and Y-ZrO_2 (31.7 mg, 36 m^2/g). Nanoparticles were prepared using the high-throughput pulsed laser ablation (HT-PLA) system, the details of which have been described recently [22]. Briefly, the HT-PLA system consists of 24 rotatable and interchangeable targets and 30 interchangeable substrates housed in a vacuum chamber with optical access to a laser beam. The laser beam (Lambda Physik Compex 100 KrF Excimer Laser, 300 mJ/pulse, 30 ns pulse duration) is then focused to a spot of ~ 0.1 cm diameter, off axis on the surface of the target, arriving at an angle of approximately 45°. Nanoparticles emanating from the target were collected on one of the flat surfaces of the support pellets (0.4 cm diameter by 0.1 cm thick cylinders) by placing the pellets inside the ablation plume at a pre-determined distance from the target. The HT-PLA vacuum chamber was maintained at 1.0 torr Ar pressure, and a grounded mask was used to prevent cross contamination of different support pellets. All PLA targets were pre-cleaned in situ by ablating the topmost layer of material onto an unused substrate.

In the first, i.e. discovery phase, a library of 35 distinct unimetallic catalytic materials was prepared by ablating pure metal targets (min 99.99% purity) that were either foils or thin disks prepared by pressing and high-temperature sintering (500 °C under Ar) powders of pure metals. For each metal, 2 sets of catalytic materials were prepared by depositing 100 laser pulses of nanoparticles onto support pellets at 2 different target-to-substrate distances. This was undertaken in order to explore the effects of nanoparticle size on selectivity and conversion, since the diameters of nanoparticles collected on substrates significantly decrease with increasing distance from the target [21, 22]. Other laser properties were maintained constant. As demonstrated earlier [22], PLA allows the synthesis of uniformly sized nanoparticles with diameters decreasing with increasing distance from the target, with a narrow particle size distribution. These features are illustrated by the transmission electron microscope (TEM) images of Rh nanoparticles shown in Fig. 1. It should be noted that the nanoparticles are deposited on the external surfaces of the pellets, with little penetration into the pores. Nanoparticles created initially will be in zero-valent metal form as they are generated in an argon atmosphere. However, upon exposure to air and/or reaction conditions, certain metals would be oxidized.

In the second phase, bimetallic catalytic materials were prepared, via sequential deposition, using the leads discovered from the reaction screening of the initial library of unimetallic catalysts. Promising bimetallic systems subsequently were investigated in greater detail in an attempt to develop superior bimetallic catalysts as well as to optimize operating conditions for the title reaction. Specifics of the sequential particle deposition processes will be described below together with the discussion of the results.

Fig. 1 TEM images of rhodium nanoparticles prepared by pulsed laser ablation. As evident from this figure, diameters of nanoparticles collected on substrates uniformly decreased with increasing distance from target at a fixed number of laser pulses (*from top to bottom*), and increased with increasing pulse numbers at a fixed distance from the target (*from left to right*) [22]. The histogram inserts illustrate a narrow particle size distribution
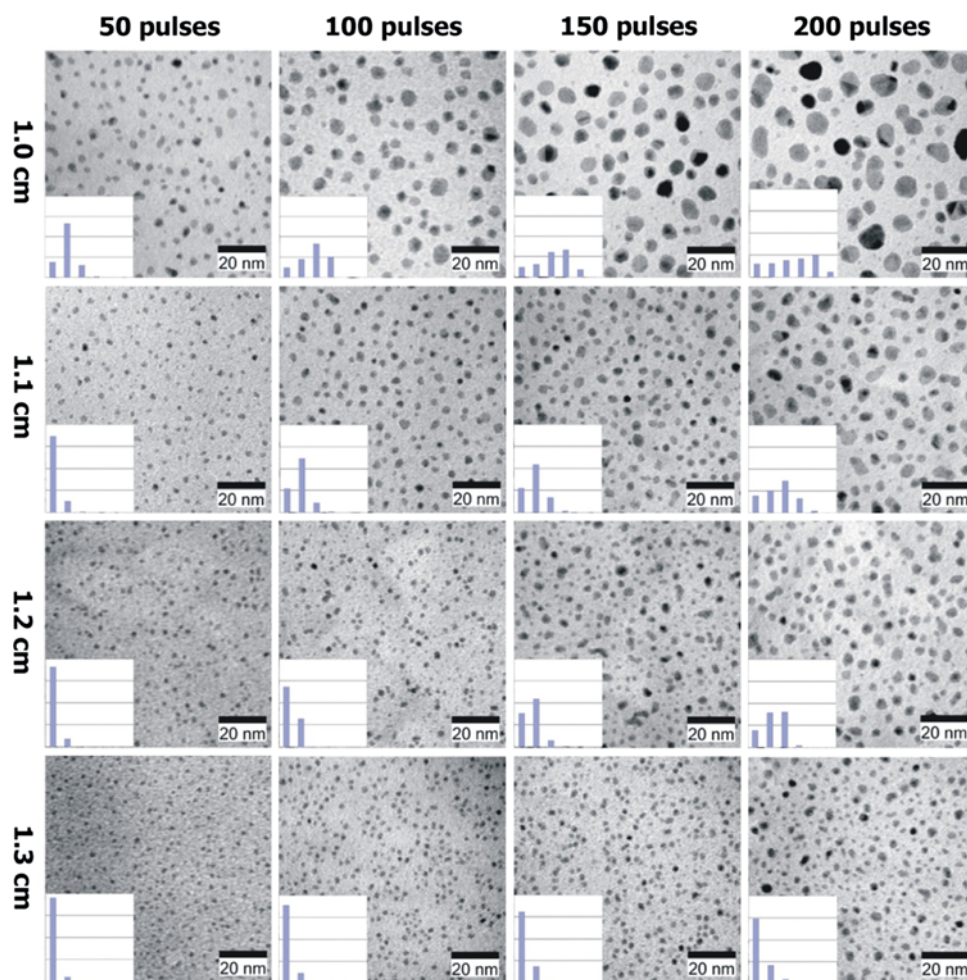

Catalyst evaluations were performed using our computer controlled array channel microreactor system described previously [18], in which up to 80 catalysts can be screened in parallel. In the array microreactors used, reactant gases flow over the flat surfaces of nanoparticle-coated support pellets which are individually isolated within reactor channels; the flow regime is similar to that of a monolithic reactor [21]. All experiments were performed under atmospheric pressure and at a gas hourly space velocity (GHSV) of 20,000 h^{-1}, representing differential reactor conditions. Initial screening experiments were performed at temperatures of 300, 333, and 367 °C using a feed gas composition of 20 vol% O_2, 20 vol% C_3H_6 and balance He. Reactor effluent gases were analyzed by withdrawing the products using a heated capillary sampling probe followed by on-line gas chromatography (Varian CP-4900 Micro GC with thermal conductivity detector, Porapak Q (10 m) and Molecular sieve 13X (10 m) columns). The propylene conversions, product selectivities, and yields (calculated as selectivity of a product × propylene conversion) of products were calculated on the basis of carbon balances. GC calibrations for propylene, oxygen, and CO_2 were performed using mass flow controllers (MKS) and He as a carrier gas. Calibrations for PO, AC, AT, and AA were performed by vaporizing known quantities of liquids in a heated, evacuated 2250 cm^3 stainless steel tank and using He as a carrier gas. All calibrations yielded linear 5-point plots with R^2 of at least 0.995, using peak area as the basis for GC calculations. Reproducibility of the experiments was well within ±10%.

3 Results and Discussion

Early scoping experiments with about 1% PO in the feed revealed that among the 5 support materials considered (i.e. g-Al_2O_3, CeO_2, SiO_2, TiO_2, and Y-ZrO_2), SiO_2 held the most promise in preserving the PO produced under the reaction conditions. This result is in harmony with the literature on propylene epoxidation catalysis [16]. Consequently, we focused our research on metal nanoparticles supported on SiO_2 (standard pellet weight 9.6 mg, BET
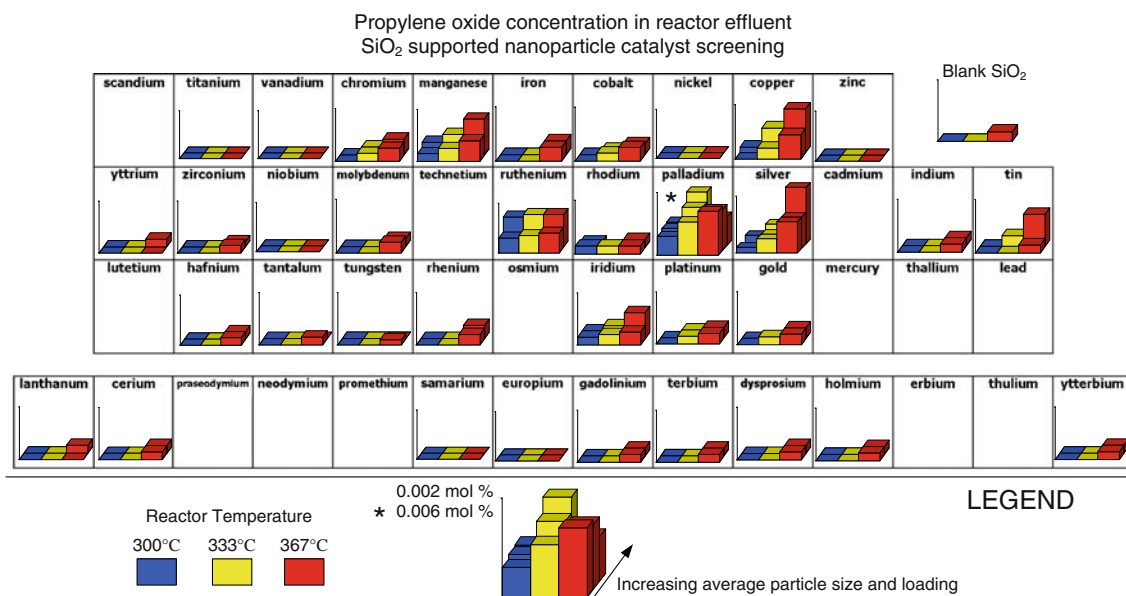
Fig. 2 Unimetallic SiO$_2$-supported nanoparticle catalyst screening results. The purpose of these experiments was to identify catalyst leads for the direct synthesis of propylene oxide from propylene and oxygen by rapidly screening large number of catalytic materials. Note: Pd catalysts produced the highest levels of PO as well as CO$_2$

area 398 m^2/g). In Fig. 2, selected results for the unimetallic nanoparticle catalyst screening experiments, completed in a time frame of about 2 weeks, are presented in a periodic table format for all of the 35 metals considered. For each element, reactor exit PO mole fractions (y-axis) are plotted as a function of temperature (x-axis). The results in the background correspond to nanoparticles collected at distances closer to the target, i.e. larger particles. In the cases of Pd and Ag, nanoparticles were collected at 3 different locations in the ablation plume.

An inspection of Fig. 2 clearly indicates SiO$_2$ supported Cr, Mn, Cu, Ru, Pd, Ag, Sn, and Ir produced the highest levels of PO among the 35 metals considered. Cu, Pd and Ag were previously reported to be active towards PO synthesis; [3–6, 14, 15] thus it is gratifying that our high throughput methods were able to confirm these earlier findings. On the other hand, Cr, Mn, Ru, Sn and Ir represent new leads of catalytic materials for the direct synthesis of PO from propylene and oxygen.

As noted earlier, the purpose of these screening experiments was to rapidly identify *new leads* for catalytic materials that promote the direct synthesis of PO via propylene and molecular oxygen. Consequently, the operating conditions for all the catalysts investigated have not been optimized; but this could be accomplished once new leads are discovered. In addition, none of the results presented in Fig. 2 are likely to have an immediate industrial impact due to low conversions and/or low selectivities attained. For example, while Pd produced PO at the highest levels among all the catalysts investigated, PO selectivity (defined

as the percent of carbon in PO among all the products) was still below 2% because of excessive CO$_2$ formation. Therefore the challenge clearly remains to increase PO production rates while also increasing PO selectivity. We addressed this need in the second phase of the program by focusing on the leads Mn and Cu, together with their binary combinations Mn + Cu. Other lead metals are currently under investigation and will be reported in the future.

Unimetallic Mn and Cu catalysts with different metal loadings were prepared by depositing nanoparticles of individual metals on the SiO$_2$ support for laser pulses from 10 to 500, while maintaining the target-to-substrate distance at 0.8 cm and other operating conditions the same as stated earlier. Based on TEM characterization of Mn and Cu nanoparticles created by PLA, the weight of catalyst collected on a 0.4 cm disc is estimated to be 30 ng Cu/pulse and 12 ng Mn/pulse at these conditions. Mn + Cu bimetallic catalysts were prepared by the *sequential deposition* process. In this case, the first set of metal nanoparticles, i.e. the under-layer, was deposited directly over the SiO$_2$ support at a fixed loading level corresponding to 500 laser pulses. This was followed by the deposition of the second metal layer (i.e. the top-layer), the loading of which was systematically varied from 10 to 500 laser pulses.

In Fig. 3, PO selectivities are presented as a function of propylene conversions for the unimetallic and bimetallic Mn and Cu catalysts explored in phase 2 at a temperature of 375 °C, GHSV of 20000 h^{-1}, and a feed gas composition of 26% C$_3$H$_6$, 14% O$_2$, and balance He. These conditions were
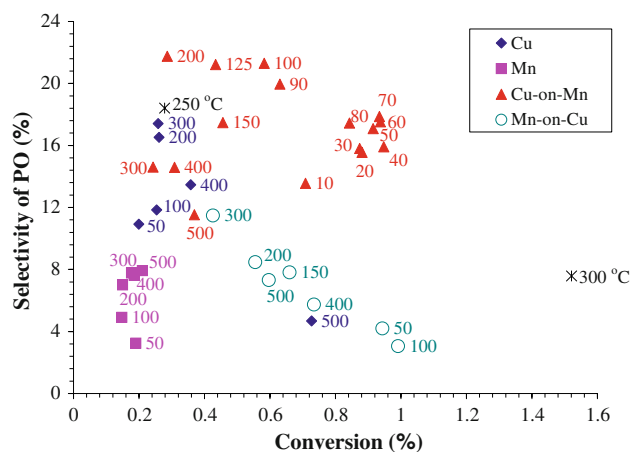
Fig. 3 Selectivity versus conversion chart at 375 °C. The numbers next to the data points represent the variable number of pulses of the topmost catalyst layer (see text). Considerable improvement of bimetallic Cu-on-Mn (*filled triangle*) catalysts is apparent when compared with unimetallic Mn (*filled square*) and Cu (*filled diamond*) catalysts. Note that Cu-on-Mn (*filled triangle*) is superior to Mn-on-Cu (*open circle*). Points indicated by temperatures (∗) correspond to 5% Cu/SiO₂ catalysts prepared by impregnation [14, 15]

found to be more favorable than the conditions used in the initial screening experiments. An inspection of Fig. 3 reveals several important results. First, both unimetallic Mn/SiO₂ (filled square) and Cu/SiO₂ (filled diamond)

catalysts exhibited inferior PO yields (PO yield = PO selectivity × Propylene conversion), regardless of the metal loading, when compared to bimetallic results discussed below. For example, the Mn/SiO₂ (filled square) data points for 10–500 laser pulses were all grouped together at the lower left side of the graph, i.e. closest to the origin. As seen from Fig. 3, PO selectivity increased slightly with Mn loading reaching a maximum of about 8% at 500 pulses (6 μg Mn). The results for Cu/SiO₂ (filled diamond) were slightly better, with PO selectivities reaching 17% at 300 pulses (9 μg Cu). However, in both cases propylene conversions were in the range of 0.2–0.4%.

The most remarkable result shown in Fig. 3 is the fact that for the bimetallic Cu-on-Mn/SiO₂ (filled triangle) catalysts *PO yields were higher by a factor of 5* than the corresponding unimetallic catalysts. These superior bimetallics exhibit PO selectivities as high as 22% at propylene conversions of 1%. This is a surprising result, since the combination of copper and manganese oxides has been used in the past as a total oxidation catalyst. [23, 24] It is also significant to note that Cu-on-Mn/SiO₂ (filled triangle) was also superior to the bimetallic Mn-on-Cu/SiO₂ (open circle) catalysts for the synthesis of PO. This result clearly demonstrates the importance of the order of deposition of the metals in bimetallic catalysts in order to affect the desired catalysis action.
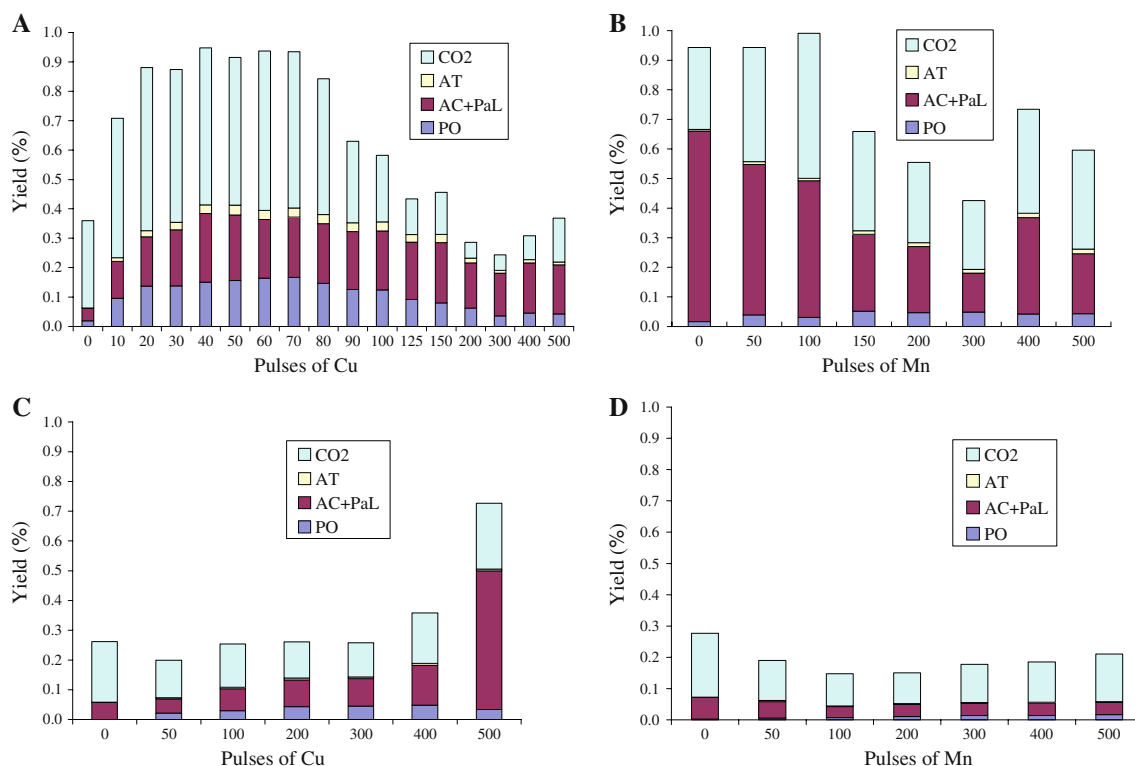
Fig. 4 Product yield results at 375 °C for (**a**): bimetallic Cu-on-Mn/SiO₂, (**b**): bimetallic Mn-on-Cu/SiO₂, (**c**): unimetallic Cu/SiO₂, (**d**): unimetallic Mn/SiO₂. The yield of PO in (**a**) is increased about 5 fold over unimetallic catalyst variations. AT = acetone, AC = acrolein, PaL = propionaldehyde (trace amounts), PO = propylene oxide

Finally in Fig. 4, the complete product yields are presented for the catalysts Cu-on-Mn/SiO$_2$ (Fig. 4a), Mn-on-Cu/SiO$_2$ (Fig. 4b), together with the same for unimetallic catalytic materials Cu/SiO$_2$ (Fig. 4c) and Mn/SiO$_2$ (Fig. 4d) at 375 °C. As evident from Fig. 4a product yields exhibit a clear optima with regard to Cu loading for the Cu-on-Mn/SiO$_2$ catalysts, with maximum PO yield observed at 70 pulses, corresponding to 2 μg Cu on 6 μg Mn. A closer inspection of Fig. 4a also shows that acrolein (AC) was the other major C$_3$ product with a selectivity of about 22%, followed by acetone (AT) at 4%. Note that the AC signal typically includes a trace amount of propionaldehyde (PaL) due to PO isomerization. However, CO$_2$ was the most abundant product formed in Cu-on-Mn/SiO$_2$ catalysis reaching selectivities in excess of 50%. These results eagerly demonstrate the need to further improve the performance of this catalytic material.

In contrast, the product mix for Mn-on-Cu/SiO$_2$ catalysts (Fig. 4b) was dominated by AC and this was entirely due to Cu being the under-layer. In fact, AC selectivities dramatically decreased from 60% on the Cu/SiO$_2$ surface (zero Mn pulses) to a value of 17% when 300 pulses on Mn were deposited. Increased coverage of the Cu sites by Mn can readily account for these results. These findings are also consistent with those observed on unimetallic Cu/SiO$_2$ catalysts (Fig. 4c), where AC selectivities steadily increased to 60% upon increasing the Cu loading to 500 pulses. It is interesting to note, however, that PO yields were not strongly influenced by the Mn loading on the Mn-on-Cu/SiO$_2$ catalysts (Fig. 4b); PO selectivities remained at about 8% above 150 pulses of Mn. Carbon dioxide still remained a significant product formed by this catalyst. Unimetallic Mn/SiO$_2$ catalysts were essentially total oxidation catalysts, with the production of only low levels of AC (Fig. 4d).

In summary, high-throughput PLA synthesis and reaction screening of supported metal nanoparticles resulted in the discovery of superior bimetallic Cu-on-Mn/SiO$_2$ catalyst leads for the direct synthesis of PO from propylene and oxygen. It has been demonstrated that multimetallic systems can exhibit synergistic catalytic effects, boosting the desired PO yields by several fold with the observed synergy depending on the sequence of deposition. This discovery calls for the undertaking of detailed follow-up studies to optimize both the catalyst preparation process and the reactor operating conditions (e.g. residence time, temperature etc.) to fully explore the limits of the Mn + Cu bimetallic system in direct PO synthesis. These results also illustrate the importance of exploring multimetallic systems and the useful role high-throughput methods play in catalyst research and development.

References

1. Matar S, Hatch LF (1994) Chemistry of petrochemical processes. Gulf Publishing Company, Houston, TX
2. Nijhuis TA, Makkee M, Moulijn JA, Weckhuysen BM (2006) Ind Eng Chem Res 45:3447–3459
3. Bettahar MM, Costentin G, Savary L, Lavalley JC (1996) Appl Catal 145:1–48
4. Monnier JR (2001) Appl Catal 221:73–91
5. Lu G, Zuo X (1999) Catal Lett 58:67–70
6. Murata K, Liu Y, Mimura N, Inaba M (2003) J Catal 220:513–518
7. Stangland E, Stavens K, Andres R, Delgass W (2000) J Catal 191:332–347
8. Sinha A, Seelan S, Akita T, Tsubota S, Haruta M (2003) Appl Catal 240:243–259
9. Wang R, Guo X, Wang X, Hao J, Li G, Xiu J (2004) Appl Catal 216:7–13
10. Yap N, Andres R, Delgass W (2004) J Catal 226:156–170
11. Zwijnenburg A, Makkee M, Moulijn J (2004) Appl Catal 270:49–56
12. Dai M, Tang D, Lin Z, Yang H (2006) Chem Lett 35:878–879
13. Chowdhury B, Juan J, Suarez B, Date M, Tsubota S, Haruta M (2006) Angew Chem Int Ed 45:412–415
14. Vaughan O, Kyriakou G, Macleod N, Tikhov M, Lambert R (2005) J Catal 236:401–404
15. Torres D, Lopez N, Illas F, Lambert R (2007) Angew Chem Int Ed 46:2055–2058
16. Song Z, Mimura N, Bravo-Suarez JJ, Akita T, Tsubota S, Oyama ST (2007) Appl Catal 316:142–151
17. Orzesek H, Schulz RP, Dingerdissen U, Maier WF (1999) Chem Eng Tech 8:691–700
18. Senkan S (2001) Angew Chem Int Ed 40:312–329
19. Senkan S, Ozturk S (1999) Angew Chem Int Ed 38:791–795
20. Senkan S, Krantz K, Ozturk S, Zengin V, Onal I (1999) Angew Chem Int Ed 38:2794–2799
21. Duan S, Kahn M, Senkan S (2007) Comb Chem High Through Screen 10:111–119
22. Senkan S, Kahn M, Duan S, Ly A, Liedholm C (2006) Catal Today 117:291–296
23. Lamb AB, Bray WC, Frazer JC (1920) J Ind Eng Chem 12:213–221
24. Musick JK, Williams FW (1974) Ind Eng Chem Prod Res Dev 13(3):175–179